Structural Eng./Earthquake Eng., JSCE, Vol. 18, No. 2, 95s—103s, 2001 July
(J. Struct. Mech. Earthquake Eng., JSCE, No. 682/ I —56)

REDUCING MESH BIAS ON FRACTURE WITHIN RIGID-BODY-SPRING NETWORKS

Jeffrey THOMURE[1], John BOLANDER Jr.[2] and Minoru KUNIEDA[3]

[1] M.S.E, Bridge Engineer, CH2M Hill
(2485 Natomas Park Drive, Suite 600, Sacramento, California 95833, USA)

[2] Member of JSCE, Ph.D., Assoc. Professor, Civil & Env. Engineering, University of California, Davis
(One Shields Avenue, Davis, California 95616-5294, USA)

[3] Member of JSCE, D. Eng., Research Associate, Dept. of Civil Engineering, Gifu University
(1-1 Yanagido, Gifu 501-1193, Japan)

Random lattice networks generally exhibit spurious heterogeneity that can overshadow important aspects of material behavior, particularly when modeling fracture in homogeneous materials. This issue is resolved through the innovative use of a crack band model for fracture within the Rigid-Body-Spring Network approach. Analyses of concrete compact tension specimens are conducted to demonstrate model objectivity with respect to size and geometry of the network components. During mode I cracking, fracture energy consumption is uniform along the crack path, independent of the meshing strategy.

Key Words: *Rigid-Body-Spring Networks, lattice models, fracture energy, crack band, Voronoi tessellation, inverse analysis, Levenberg-Marquardt minimization*

1. INTRODUCTION

Lattice models are an effective means for studying the fundamental aspects of fracture in various natural and engineered materials[1]. In particular, lattice models have been used to study the process of fracture localization and macroscopic softening of quasi-brittle materials, such as concrete[2),3)]. The lattices are typically formed from basic mechanical elements, such as central-force springs or beam-springs, which are interconnected at nodal sites. The distribution of nodal sites is often regular, so that each site has the same coordination number. However, random site distributions are preferred for some applications since random geometry networks have exhibited less mesh bias with respect to potential cracking directions[4)].

Fracture is represented by breaking the springs according to simple rules, which are typically defined local to the lattice element axes. Commonly, a measure of stress is determined from spring axial force (and moments in beam-springs), which is then used within criteria for deciding crack initiation and propagation. As shown in this paper, lattice elements that are oriented skew to the prevailing loading direction tend to provide excessive strength and toughness during fracture, similar to the stress locking that occurs in finite element models with smeared cracking[5)]. Consequently, local fracture energy consumption varies greatly during crack advance through random networks. Although disorder in actual materials causes fluctuations in strength and toughness, the spurious heterogeneity arising from network geometry is undesirable in that it bears no connection to actual material features and, as will be shown later, can lead to unrealistic results. One general goal is to remove mesh bias on fracture so that disorder can be implemented in a rational manner, either by explicit or probabilistic means. Reduction of mesh bias has been accomplished in finite element models of softening materials using various sophisticated approaches, including the use of:

- nonlocal and higher-order continuum theories[6),7),8)],
- a displacement (or displacement gradient) jump embedded within the element shape

functions[9),10),11)], or

- adaptive remeshing about the crack tip region[12),13)].

As noted above, smeared crack finite element models of fracture in softening materials generally exhibit stress locking[5)]. The problem can be severe even for mode I type cracking when the crack runs skew to the principle directions of a regular mesh or, more generally, when the crack traverses a mesh based on irregular geometries, such as those constructed using random numbers. The use of random geometries to discretize the domain is attractive in that it facilitates automatic mesh generation.

In this work, fracture is modeled using a Rigid-Body-Spring Network (RBSN), which is a special type of random lattice network[14)]. More specifically, the crack band concept[15)] is implemented within the RBSN to obtain uniform fracture energy consumption along the principal crack trajectory, independent of network size and geometry. The technique is demonstrated through analyses of concrete fracture specimens. As mentioned, concrete materials exhibit softening behavior during tensile cracking[16),17)]. To relate this demonstration to actual test results, the material softening relations used in the analyses are determined through an inverse analysis procedure that utilizes Levenberg-Marquardt minimization.

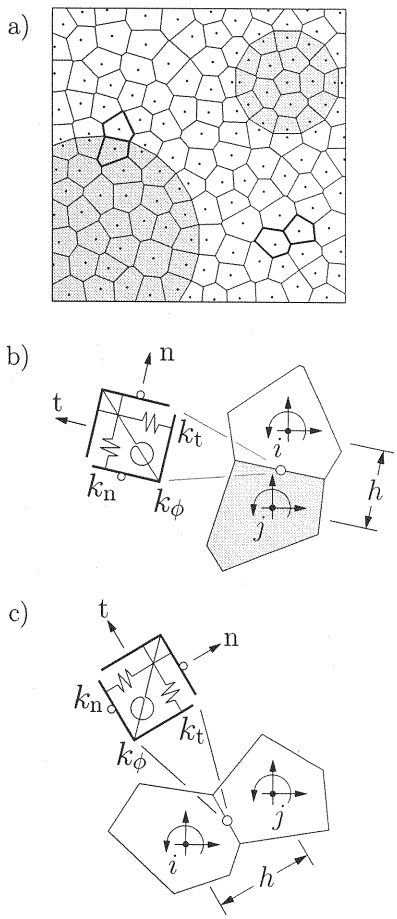

Fig. 1 RBSN model: a) Voronoi discretization of a multi-phase material; b) basic elemental unit along material interface; and c) basic elemental unit within homogeneous phase

2. THE RBSN APPROACH

The RBSN is based on the Rigid-Body-Spring Model (RBSM) developed by Kawai[18)]. In the RBSN approach, the material domain is discretized using a Voronoi diagram[19)] on a set of randomly distributed points, or nuclei (**Fig. 1**); network degrees of freedom are defined at the nuclei. System flexibility is lumped into zero-size spring sets that interconnect the rigid Voronoi cells along their common boundary segments. Each spring set consists of a normal, tangential, and rotational spring oriented local to the boundary segment. Spring stiffnesses are scaled in proportion to the distance between the cell nuclei, h, and the length of the common boundary segment, ℓ, in a manner that represents the elastic properties of the continuum[18),20)]. System equilibrium equations are constructed from each elemental unit (i.e. each two-cell subassembly) using the direct stiffness method.

Tensile fracture within the RBSN is represented using the crack band concept of Bažant and Oh [15)]. For each load step, and during equilibrium iterations, the forces in the spring sets are determined from the displacement solution. Average measures of normal and tangential stress are computed by dividing the corresponding spring set force components by the associated boundary segment area. The strength and fracture energy properties of each spring set are defined according to a softening diagram, such as that shown in **Fig. 2**, where σ is crack normal stress and w is the crack opening displacement.

The elastic properties of critical spring sets are degraded through a series of fracture events. The ratio R of normal stress to initial strength (or to residual strength defined by the soft-

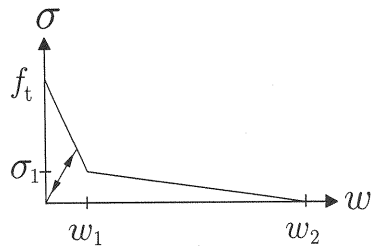

Fig. 2 Bilinear softening diagram

ening curve after crack initiation) defines the criticality of each spring set. As is common for lattice models, only the spring set with the greatest $R \geq 1$ undergoes fracture during a computational cycle. With each fracture event, spring forces are released in accordance with the softening relation, which produces an inbalance between the external and internal nodal force vectors. Conventional Newton-Raphson type iterations are performed to eliminate the out-of-balance forces to within a preset tolerance. Such convergence is required before incrementing the external forces and/or displacements.

Specific fracture energy, G_F, is equal to the area under the stress versus opening displacement diagram (i.e., the energy consumption per unit area of crack formation). To realize constant fracture energy consumption for different cell sizes, damage is assumed to be uniformly distributed over the element length according to the crack band concept[15]. Strain values characterizing the softening response are dependent on crack band width:

$$\epsilon^{cr} = \frac{w}{h} \tag{1}$$

where ϵ^{cr} is the crack strain and h is the crack band width, defined as the distance between contiguous cell nuclei. This definition implies that the crack band forms parallel to the boundary segment and has the dimensions shown in **Fig. 3a**.

3. NETWORK GEOMETRY BIAS ON FRACTURE

When modeling heterogeneous materials, the geometry of the network either:

1. corresponds to specific features of the material structure, such as an interface between different phases of a composite material like concrete (**Fig. 1b**); or

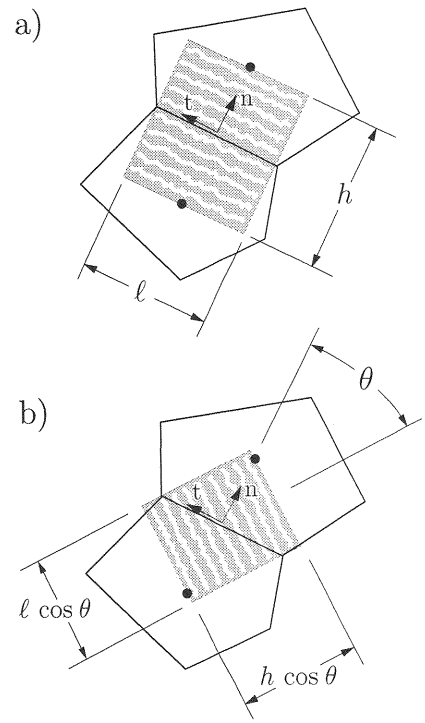

Fig. 3 Crack band orientation and dimensions for: a) band direction parallel to boundary segment; and b) band direction defined by angle θ

2. is not related to any material feature, such as when representing homogeneous properties within a single phase (**Fig. 1c**).

In most lattice models, including previous applications of the RBSN approach[14),21)], the fracture properties depend on element orientation with respect to the loading direction. For example, lattice element fracture criteria often contain an axial force term. As shown by the following example, such models are not well-suited for modeling arbitrary crack movement in homogeneous media (i.e. case 2 above).

Figure 4 shows a two-cell assembly loaded under controlled axial displacement. The relative displacement between the two nuclei in the direction of loading is δ; the average stress over the assembly cross-section (taken perpendicular to the direction of loading) is denoted by $\overline{\sigma}$. The stress acting normal to the boundary segment is

$$\sigma_n = \frac{F_n}{t\,\ell} \tag{2}$$

where F_n is the force in the spring oriented normal to the boundary segment and t is the

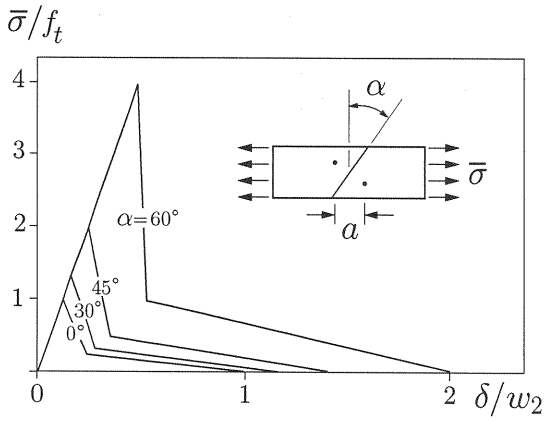

Fig. 4 Uniaxial tension analyses

material thickness. The fracture criterion is based on σ_n, in conjunction with the softening relation shown in **Fig. 2**.

Load-displacement curves are produced for boundary segment inclinations ranging from $\alpha = 0°$ to 60° (**Fig. 4**). Length a is the distance between the nuclei in the direction of loading; its value is held constant as one means for interpreting the effects of α. Peak load, $\overline{\sigma}_{\max}$, and traction-free crack width, δ_0, are simple functions of α[22], both increasing with larger α.

$$\overline{\sigma}_{\max} = f_t \ \sec^2 \alpha \tag{3}$$

and

$$\delta_0 = w_2 \ \sec \alpha, \tag{4}$$

where f_t is the uniaxial tensile strength of the material and w_2 is the traction free opening in the direction normal to the common boundary segment. Clearly, fracture energy consumption depends on the boundary segment orientation with respect to the principal tension direction. This is precisely the type of bias present in lattice models that rely on element axial force terms within the fracture criteria.

4. AN OBJECTIVE FRACTURE CRITERION

Consider crack band orientation as defined by angle θ with respect to the element axis (**Fig. 3b**). The crack band width is $h \cos\theta$, which is the distance between the corresponding cell nuclei in the direction defined by θ. The crack band length is $\ell \cos\theta$. Angle θ can be determined so that fracture runs perpendicular

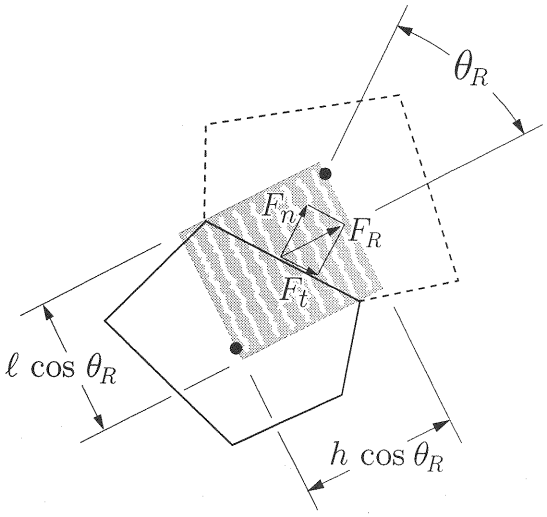

Fig. 5 Crack band model for objective fracture criterion

to the direction of major principle tensile stress, as supplied by an algorithm for computing tensorial stress measures within the RBSN[20]. For the tensile type loadings considered here, the following alternative approach is used.

Figure 5 shows normal and tangential spring set forces for a two-cell assembly. The crack band is assumed to form perpendicular to the resultant of this force pair, F_R. The average stress acting over the crack band is

$$\sigma_R = F_R/(t \ \ell \cos\theta_R). \tag{5}$$

The stress σ_R is compared with the current strength of the spring set, defined by the softening relation, to determine the criticality of the spring set. If the direction of force resultant approaches that of the boundary segment (i.e., if $|\theta_R|$ approaches $\pi/2$), then the denominator in Eq. (5) goes to zero. This is generally not a problem because F_R also diminishes, if the stress state is primarily uniaxial tension. However, to avoid potential difficulties, especially when $|\theta_R| \approx \pi/2$, a minimum threshold is set on the $\cos\theta_R$ term.

Using this approach, the load displacement curves produced for the specimen in **Fig. 4** are independent of α and match the results for $\alpha = 0$. Moreover, this approach preserves proper fracture energy consumption under changes in both mesh size and geometry, as demonstrated in the next section.

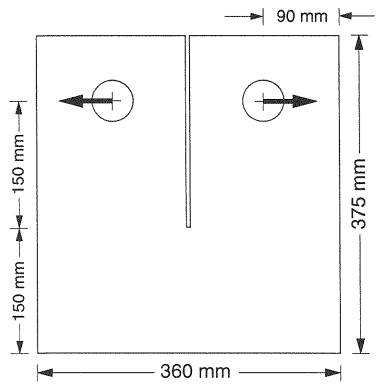

Fig. 6 CT specimen configuration[23)]

5. MODEL APPLICATION

(1) Problem description

Objectivity of the new fracture criterion is demonstrated through analyses of concrete compact tension (CT) specimens. The experimental results produced by Wittmann *et al.*[23)] are used for comparison. The specimen configuration is shown in **Fig. 6**. Two varieties of discretization are considered here: 1) one that anticipates the crack trajectory with a straight line discretization along the ligament length, and 2) one that uses a random geometry discretization of the ligament, so as not to anticipate cracking direction (**Fig. 7**). Both specimens are based on nearly the same average cell density in the ligament region.

(2) Inverse analysis of softening parameters

The parameter values for the bilinear softening relation (i.e., f_t, σ_1, w_1, and w_2 in **Fig. 2**) are determined through an inverse analysis procedure, which maximizes the correlation between the numerical and experimental curves representing load versus crack mouth opening displacement (CMOD). For any given CMOD, represented by Δ in **Fig. 8**, there is typically a difference, or error, between the calculated and measured reactive forces. An optimal set of parameters can be extracted by minimizing the square of this error over a length of the response curve (e.g., for Δ ranging from 0 to a maximum opening, Δ_0). A Levenberg-Marquardt algorithm is used to minimize the

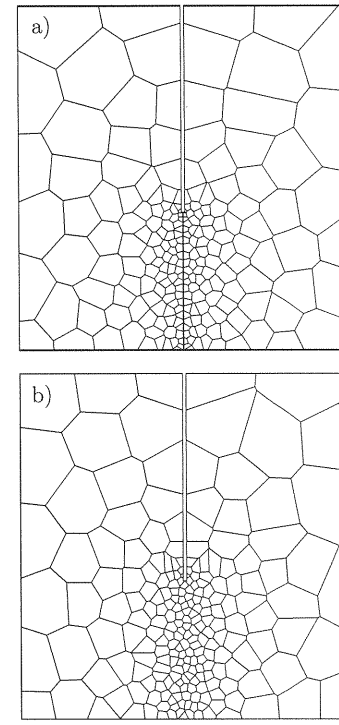

Fig. 7 Mesh designs: a) straight line discretization along ligament length; b) random discretization along ligament length

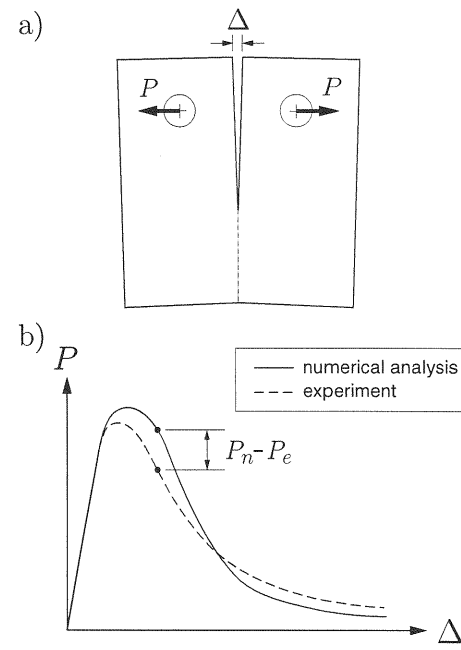

Fig. 8 Inverse analysis of softening parameters

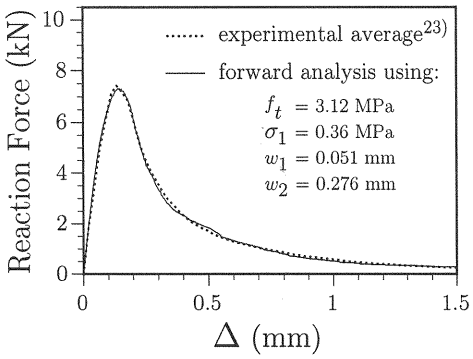

Fig. 9 Forward analysis results using extracted softening parameter set

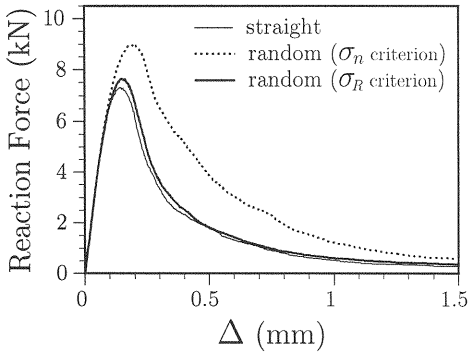

Fig. 10 Load versus CMOD diagrams for different modeling strategies

following functional relation[22)]:

$$\mathcal{F}(f_t,\sigma_1,w_1,w_2) = \int_0^{\Delta_0} [P_n(f_t,\sigma_1,w_1,w_2) - P_e]^2 \, \mathrm{d}\Delta \quad (6)$$

where P_n and P_e represent the numerical and experimental reactive forces, respectively. To determine the softening parameter set for the analyses that follow, this procedure was applied using the CT specimen with the embedded straight crack path. Using the derived parameter set, shown in **Fig. 9**, a forward analysis reproduces the experimental result. Alternative methods for inverse analysis of the softening parameters are described elsewhere[24),25),26)].

(3) Load-CMOD response

Using the random discretization over the ligament region, the CT specimen is analyzed using the fracture criteria based on σ_n and σ_R, as determined from eqs. (2) and (5), respectively. Load-CMOD curves produced by each analysis are compared with the benchmark case result (i.e., that obtained from the embedded straight crack path) in **Fig. 10**. The results from the σ_n criterion exhibit higher peak load and increased energy consumption in the post-peak regime of the loading history. On the other hand, the σ_R criterion results agree well with those of the benchmark case. The slight differences between the results of the σ_R criterion and the benchmark case are due to the non-horizontal action of σ_R for spring sets located off the plane of symmetry, especially near the prenotch tip. Fixing angle θ for each spring set so that the crack band is vertical yields results that are identical to the benchmark case.

Analyses based on different realizations of the random geometries produce the results shown in **Fig. 11**. Using the σ_n criterion, analyses exhibit significant scatter in the results. Using the σ_R criterion, however, consistent results are obtained. The reasons for this behavior can be explained by examining energy consumption along the crack trajectory.

(4) Fracture energy consumption

Each discrete fracture event consumes an amount of energy, which can be computed from the change in reactive force at the load points for that computational cycle. The energy value and the associated spring-set number are stored in memory for later use in a post-processing module, so that the distribution of local energy consumption, g_F, can be viewed at any load stage. **Figure 12** shows distributions of energy consumption (up through a load point displacement of 2.25 mm) for the specimens with straight crack and random crack geometries. Each segment of the energy distribution plot corresponds to a damaged spring set. The energies have been normalized by G_F, the area under the bilinear softening diagram used for the analyses (**Fig. 2**). The thicknesses of the lines indicating cracking are scaled in proportion to crack opening displacement. Minor damage occurs outside of the crack band, yet such information does not appear in the graphics since the corresponding opening displacements and energy consumptions are orders of magnitude less than those of the crack band.

As expected, the straight crack analysis produces uniform energy consumption along the crack trajectory. In contrast, the random geom-

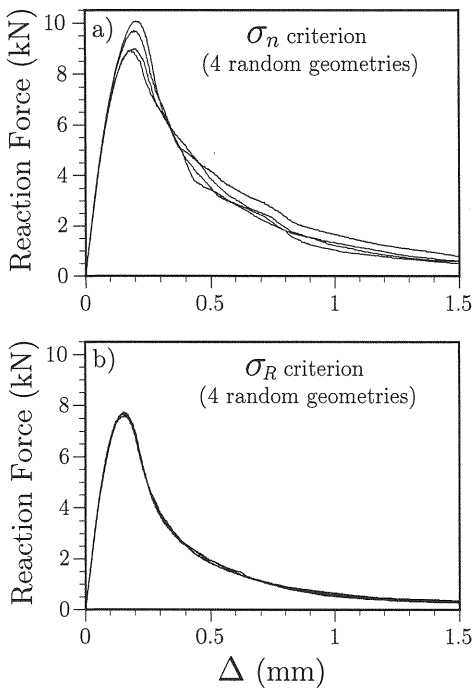

Fig. 11 Analysis results for different random realizations of network geometry

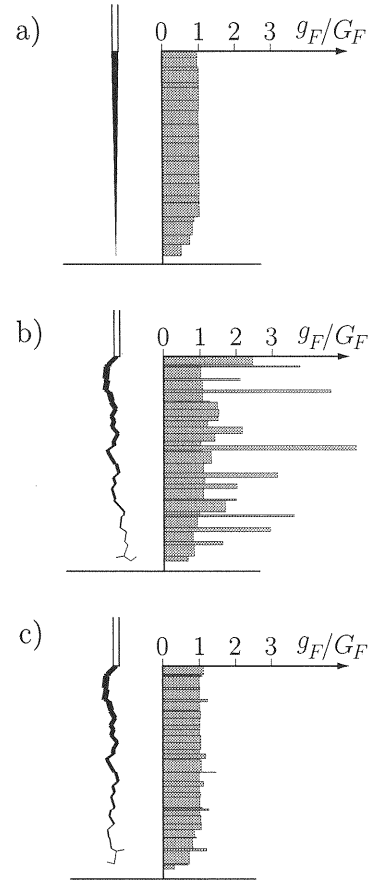

Fig. 12 Fracture energy distributions along ligament length for: a) embedded straight crack path; b) random discretization (σ_n criterion); c) random discretization (σ_R criterion)

etry analysis based on the σ_n criterion exhibits large variations in energy consumption over the ligament length, which may be viewed as artificial heterogeneity of the network. Elements with boundary segments that are nearly in line with the preferential crack direction consume fracture energy $g_F \approx G_F$, while those oriented at larger angles consume a proportionally greater amount of energy. This form of locking can cause the damage band to broaden and is not compatible with the use of a softening relation derived from inverse analysis. This problem with element locking can be partially avoided through the use of a fracture surface in stress space (e.g., a Mohr-Coulomb surface[21]), yet the physical interpretation of such a model is unclear.

For the random geometry analysis based on the σ_R criterion, the energy distributions are nearly uniform along the principal crack trajectory, with $g_F \approx G_F$. (Fixing θ to achieve a vertical crack band for each spring set yields $g_F = G_F$ over the ligament length.) Crack propagation through the random mesh produces practically the same results as crack propagation along a smooth, predefined pathway. This is desirable in that the random geometry does not represent any structural features within the material, but rather has been used to facilitate discretization of the domain.

(5) Observations

The reduction of stress locking in continuum finite elements is complicated due, in part, to the dependence of element cracking on multiple nodal points: at least three nodes affect cracking within planar finite elements, while at least four nodes affect cracking within volume elements for three-dimensional analysis. In contrast, the modeling of material separation within a RBSN element involves only two nodal points, even when extending the analysis framework to three dimensions. For the mode I openings considered here, stress locking is effectively eliminated using the simple concept outlined in **Sec. 4** (i.e., the use of a crack band directed perpendicular to

the tension force resultant of the corresponding spring set). Both the crack initiation and crack propagation criteria are invariant with respect to the local geometry of the lattice, which has important implications for the lattice modeling of fracture, in general.

Nonlinear fracture mechanics models are practical because the complex mechanisms of the fracture process are not explicitly modeled, but rather are treated from an energy balance perspective. Here, through the use of the crack band approach[15], the softening relation accounts for the various toughening mechanisms active during concrete fracture, such as distributed microcracking, resistance to separation of tortuous surfaces, and crack face bridging. The crack band modeling of fracture also applies when there is no abrupt change in geometry, such as a prenotch, to promote fracture initiation. For example, the RBSN approach has been successful in modeling distributed cracking (including crack spacing and crack widths) over the constant moment region of structural concrete members[21),27].

The fracture model presented in this paper is applicable when the local stress state is primarily uniaxial tension. Although this capability is important for a variety of material and structural analyses, many of the research needs in structural concrete involve compressive failure and/or fracture under multi-axial loadings. Current work involves extending the RBSN modeling of fracture to handle more general loading cases.

6. CONCLUSION

For most lattice models, fracture depends on the orientation of the lattice components with respect to the governing tension field. The resulting local variations in strength and toughness can be viewed as artificial heterogeneity of the lattice network. Such behavior is often problematic, particularly when modeling crack propagation through homogeneous media, where the lattice component geometry and orientation bear no relation to any specific features of the material.

In this work, objectivity with respect to network component geometry has been achieved through the innovative use of a crack band model within the RBSN approach. Analyses of concrete CT specimens have been used to demonstrate the method's ability to realize uniform fracture energy consumption during mode I cracking, independent of the mesh design. This basic result for the homogeneous case is applicable to many types of concrete analysis and is a starting point for more rational representations of heterogeneity, either by explicit or probabilistic means. Since this new method eliminates mesh bias on cracking, one of the primary motivations for using random lattices has been removed. The issue of whether to use regular or random lattices should be revisited.

REFERENCES

1) *Statistical Models for the Fracture of Disordered Media,* Herrmann, H.J. and Roux, S. eds., Elsevier/North Holland, Amsterdam, 1990.

2) Schlangen, E. and van Mier, J.G.M.: Experimental and numerical analysis of micromechanisms of fracture of cement-based composites, *Cem. Conc. Composites*, Vol. 14, pp. 105-118, 1992.

3) van Mier, J.G.M.: *Fracture Processes of Concrete*, CRC Press, Boca Raton, Florida, 1998.

4) Schlangen, E. and Garboczi, E.J.: New method for simulating fracture using an elastically uniform random geometry lattice, *Int. J. Engng. Sci.*, Vol. 34, No. 10, pp. 1131-1144, 1996.

5) Rots, J.G.: Stress rotation and stress locking in smeared analysis of separation, in *Fracture Toughness and Fracture Energy - Test Methods for Concrete and Rock*, Mihashi, H., Takahashi, H. and Wittmann, F.H. eds., Balkema, Rotterdam, pp. 367-382, 1989.

6) Pijaudier-Cabot, G. and Bažant, Z.P.: Nonlocal damage theory, *J. Engng. Mech.*, ASCE, Vol. 113, No. 10, pp. 1512-1533, 1987.

7) Bažant, Z.P. and Lin, F.-B.: Nonlocal smeared cracking model for concrete fracture, *J. Struct. Engng.*, ASCE, Vol. 114, No. 11, pp. 2493-2510, 1988.

8) de Borst, R. and Mühlhaus, H.B.: Continuum models for discontinuous media, in *Fracture Processes in Concrete, Rock and Ceramics*, van Mier, J.G.M., Rots, J.G. and Baker, A. eds., Spon/Chapman & Hall, London, pp. 601-618, 1991.

9) Ortiz, M., Leroy, Y. and Needleman, A.: A finite element method for localized failure analysis, *Comp. Methods Appl. Mech. Engng.*, Vol. 61, pp. 189-214, 1987.

10) Klisinski, M., Runesson, K. and Sture, S.: Finite element with inner softening band, *J. Engng. Mech.*, ASCE, Vol. 117, No. 3, pp. 575-587, 1991.

11) Oliver, J.: Modelling strong discontinuities in solid mechanics via strain softening constitutive equations, *Int. J. Num. Meth. Engng.*, Vol. 39, pp. 3575-3624, 1996.

12) Bocca, P., Carpinteri, A. and Valente, S.: Size effects in the mixed mode crack propagation - Softening and snap-back analysis, *Engng. Fracture Mech.*, Vol. 35, pp. 159-170, 1990.

13) Ingraffea, A.R. and Saouma, V.: Crack growth prediction in scaled down model of concrete gravity dam, *Theoretical and Applied Fract. Mech.*, Vol. 21, pp. 29-40, 1994.

14) Bolander, J.E. and Saito, S.: Fracture analysis using spring networks with random geometry, *Engng. Fracture Mech.*, Vol. 61, No. 5-6, pp. 569-591, 1998.

15) Bažant, Z.P. and Oh, B.H.: Crack band theory for fracture of concrete, *Materials and Structures*, RILEM, Paris, Vol. 16, pp. 155-176, 1983.

16) JCI Technical Committee on Fracture Mechanics of Concrete: *JCI Colloquium on Fracture Mechanics of Concrete Structures*, Japan Concrete Institute, JCI-C19, 1990.

17) ACI Committee 446: Fracture mechanics of concrete - Concepts, models and determination of material properties, in *Fracture Mechanics of Concrete Structures*, Bažant, Z.P. ed., Elsevier Applied Science, London, pp. 1-140, 1992.

18) Kawai, T.: New discrete models and their application to seismic response analysis of structures, *Nuclear Engng. Design*, Vol. 48, pp. 207-229, 1978.

19) Okabe, A., Boots, B. and Sugihara, K.: *Spatial Tessellations - Concepts and Applications of Voronoi Diagrams*, John Wiley & Sons, Chichester, England, 1992.

20) Bolander, J.E., Yoshitake, K. and Thomure, J.: Stress analysis using elastically uniform rigid-body-spring networks, *J. Struct. Mech. Earthquake Engng.*, JSCE, No. 633/I-49, pp. 25-32, 1999.

21) Bolander, J.E., Hong, G.S. and Yoshitake, K.: Structural concrete analysis using rigid-body-spring networks, *J. Comp. Aided Civil and Infrastructure Engng.*, Vol. 15, pp. 120-133, 2000.

22) Thomure, J.: Modeling tension and compression failures in concrete materials, M.S. degree thesis, Department of Civil and Environmental Engineering, University of California, Davis, U.S.A., 2000.

23) Wittmann, F. H., Mihashi, H. and Nomura, N.: Size effect on fracture energy of concrete, *Engineering Fracture Mechanics*, Vol. 35 (1/2/3), pp. 107-115, 1990.

24) Roelfstra, P.E. and Wittmann, F.H.: Numerical method to link strain softening with failure of concrete, in *Fracture Toughness and Fracture Energy of Concrete*, Wittmann, F.H. ed., Elsevier Science Publishers, Amsterdam, pp. 163-175, 1986.

25) Nanakorn, P. and Horii, H.: Back analysis of tension-softening relationship of concrete, *Proc. Japan Soc. Civil Engs.*, No. 544/V-32, pp. 265-275, 1996.

26) Kitsutaka, Y.: Fracture parameters by polylinear tension-softening analysis, *J. Engng. Mech.*, ASCE, Vol. 123, No. 5, pp. 444-450, 1997.

27) Bolander, J.E. and Le, B.D.: Modeling crack development in reinforced concrete structures under service loading, *J. Constr. Bldg. Materials*, Vol. 13, Nos. 1-2, pp. 23-31, 1999.

(Received September 19, 2000)